ELSEVIER

Journal of Nuclear Materials 307–311 (2002) 1052–1056

journal of nuclear materials

www.elsevier.com/locate/jnucmat

Decay heat measurement of fusion related materials in an ITER-like neutron field

Y. Morimoto *, K. Ochiai, F. Maekawa, M. Wada, T. Nishitani, H. Takeuchi

Fusion Neutronics Laboratory, Japan Atomic Energy Research Institute, Tokai-mura, Naka-gun, Ibaraki-ken 319-1195, Japan

Abstract

Decay heat is one of the most important factors for the safety aspect of ITER. Especially, the prediction of decay heat with an uncertainty less than 15% for the three most important materials, i.e., copper, type-316 stainless steel (SS316) and tungsten, is strongly requested by designers of ITER. To provide experimental decay heat data needed for validation of decay heat calculations for SS316 and copper, an experiment was conducted as the ITER/EDA task T-426. An ITER-like neutron field was constructed, and decay heat source distributions in thick copper and SS316 plates were measured with the whole energy absorption spectrometer. The measured decay heat distributions in the thick sample plates were compared with the predicted values by MCNP calculations. It was found that the use of an effective activation cross-section calculated by MCNP was needed to consider the self-shielding effects and, for both cases, MCNP calculations could predict the decay heat adequately.

1. Introduction

Decay heat is one of the most important factors for the safety aspect of ITER. An accurate decay heat prediction for various materials found in ITER is required to reduce safety design margins. Especially, the prediction of decay heat with an uncertainty less than 15% for the three most important materials, i.e., copper, type-316 stainless steel (SS316) and tungsten, is strongly requested by the designers of ITER. To provide experimental decay heat data necessary for validation of decay heat calculations for the tungsten baffle plates, an irradiation experiment was conducted at the Fusion Neutronics Source (FNS) facility at Japan Atomic Energy Research Institute [1]. In this experiment the main attention was focused on the accuracy of the self-shielding effect of the $^{186}W(n,\gamma)^{187}W$ reaction induced by low-energy neutrons and the results show that the precise treatment of the self-shielding is necessary for an accurate prediction of decay heat for tungsten.

As the decay heat sources of copper and SS316 are also generated by the resonance reactions, a supplemental experiment was conducted as an ITER/EDA task T-426 to provide experimental decay heat data needed for the validation of decay heat calculations for copper and SS316 in an ITER-like neutron field. This report summarizes these decay heat experiments.

2. Experiment

2.1. Simulation of ITER-like neutron field

One of the important features of the experiment is the simulation of the neutron field environment at the baffle plates of ITER. A neutron spectrum calculated by Sawan et al. [2] was employed as a reference ITER-like spectrum. Their calculation took full details of geometrical configuration of ITER into account by a precise three-dimensional ITER model with the MCNP-4A Monte Carlo neutron transport code [3]. The neutron spectrum was calculated just at the position of the baffle

* Corresponding author. Tel.: +81-29 282 6818; fax: +81-29 282 5709.

E-mail address: morimoto@fnshp.tokai.jaeri.go.jp (Y. Morimoto).

0022-3115/02/$ - see front matter © 2002 Published by Elsevier Science B.V.
PII: S0022-3115(02)01296-5

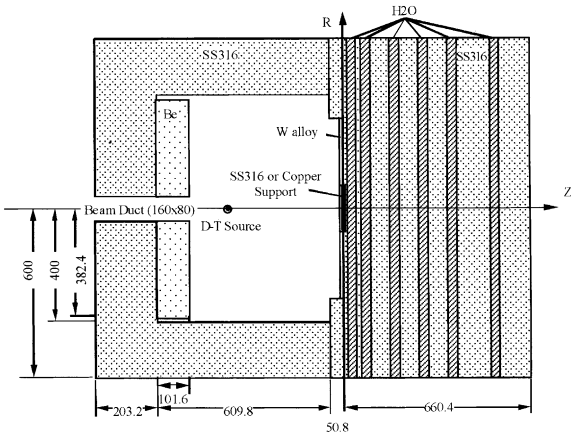

Fig. 1. Cross-sectional view of the experimental assembly for the ITER-like neutron field. The geometry is in an R–Z symmetry except for the beam ducts and the pure-tungsten.

plates, therefore, the calculated reference spectrum was believed to be very close to the real neutron spectrum appeared in ITER. We attempted to reproduce the reference spectrum by using the D–T neutron source of FNS. Most parts of the final experimental assembly shown in Fig. 1 were in cylindrical symmetry. A beryllium reflector of 382.4 mm in radius and 101.6 mm in thickness was introduced in to the source reflector made of SS316. A tungsten layer was attached on the front surface of the SS316/water region. A central part of the tungsten layer was SS316 plate or copper plate of $254 \times 254 \times 12.6$ mm^3 for each decay heat measurement, while surrounding parts of the tungsten layer were made by many tungsten-alloy tiles of $50.7 \times 50.7 \times 12.6$ mm^3.

2.2. Sample preparation and irradiation

Another important feature of the experiment is the observation of the self-shielding effect of neutron fluxes in the sample plate of 12.6 mm in thickness.

The copper plates had thicknesses from 0.1 to 1 mm. On the other hand, copper samples for decay heat measurements were thin copper foils, area of 25×25 mm^2, 25 μm in thickness and 140 mg in weight. The 16 copper plates were stacked. Fifteen samples were sandwiched by each pair of copper plates, and also two samples were attached on the front and rear copper plates.

The SS316 plate and the copper plate of 254×254 mm^2 had a square space of 45×45 mm^2 at their center. The space was filled with 13 SS316 plates of 45×45 mm^2 for decay heat measurement of SS316 and with 16 copper plates of 45×45 mm^2 for decay heat measurement of copper. The SS316 plates had a thickness of 1 mm. On the other hand, SS316 samples for decay heat measurement were very thin SS316 foils, area of 25×25 mm^2, 7.5 μm in thickness and 37 mg in weight. The 13 SS316 plates were stacked. Twelve samples were sandwiched by each pair of SS316 plates, and also two samples were attached on the front and rear SS316 plates.

A neutron irradiation was conducted for 420 min with a total neutron intensity of 5.83×10^{15} for copper samples and as 3.01×10^{15} for SS316 samples. A number of D–T neutrons generated at the target were determined by the associated alpha-particle counter with an accuracy of 2%. The alpha-counts were recorded for every 10 s by a multi-channel scaling system to monitor fluctuation of numbers of generated neutrons.

2.3. Decay heat measurements

After irradiation, the decay heat in each foil sample was measured by the whole energy absorption spectrometer [4–6]. Decay heat data for copper samples were obtained at cooling times of approximately 0.5 days after the end of irradiation. The measurements were repeated two days after the first measurements to follow the time evolution of decay heat. Note that the half-life of ^{64}Cu is 12.7 h. The measurements for SS316 samples were repeated at 2 and 15 h after the end of the irradiation to follow the time evolution of decay heat. Note that the half-life of ^{56}Mn is 2.579 h.

3. Experiment analysis

The continuous energy Monte Carlo transport calculation code MCNP-4B was employed for the experiment analyses. The code could treat precisely the self-shielding effect for resonance reactions. Cross-section data used for the neutron transport calculation were taken from FENDL/2 [7]. The experimental assembly including the very fine sample plates/foils stack and the D–T neutron source conditions were modeled precisely. Neutron spectra and the activation reaction rates in the VITAMIN-J 175-energy bins were calculated at each sample position.

Decay heat values averaged in the thick sample plates were calculated with the ACT4 code, which is the inventory calculation module of the THIDA code system [8], by using the calculated neutron fluxes. An activation cross-section library that had been processed into 175 groups from FENDL/A-2.0 [9] without taking into account of self-shielding effect was also used.

4. Results and discussion

4.1. Decay heat of copper

Measured pulse height spectra by WEAS clearly demonstrate that the main contributor of decay heat is

^{64}Cu. Two peaks corresponding to β decay of ^{64}Cu below 578.2 keV and electron capture below 1674.9 keV were clearly observed. Gradients of decay curves for the copper samples were consistent with the expected gradient with a half-life of 12.7 h. This is an another experimental proof that most of the measured decay heat is contributed by ^{64}Cu.

Measured data for all samples were converted to decay heat values at the cooling time of 16 h. Since the total measurement time of ≃1 h for all the samples was not negligible compared to the half-life of ^{64}Cu of 12.70 h, the derived decay heat at the time of each measurement was extrapolated to a common time with assuming the decay half-life of 12.7 h. The decay heat distribution in the thick copper plate and the calculated production rates of ^{64}Cu were shown in Fig. 2. Both experimental and calculated spatial distributions are normalized for comparisons so that the spatial average is unity. It is obvious that the spatial distribution by calculation agrees nicely with the experimental distribution (within ≃5%). This results suggests that the change of the decay heat distribution in the copper plate due to self-shielding effect can be reproduced by MCNP calculations which use point-wise cross-section data.

The averaged value of the measured decay heat value was compared with the calculated decay heat value with the neutron flux averaged over the thick copper plates. The C/E values of the decay heat of copper were 1.72 when the self-shielding effect of the ^{63}Cu(n,γ)^{64}Cu reaction was included in the calculation and 1.15 when the self-shielding effect of the ^{63}Cu(n,γ)^{64}Cu reaction was not included in the calculation.

Fig. 3 shows effective ^{63}Cu(n,γ)^{64}Cu reaction cross-sections at the two positions, which are derived by dividing the group-wise reaction rates by the group-wise neutron fluxes. The effective cross-section at 500 eV is largely decreased by nearly one order of magnitude due to the self-shielding effect. This is the reason why the reaction rates of the ^{63}Cu(n,γ)^{64}Cu reaction are small at the center of copper plates.

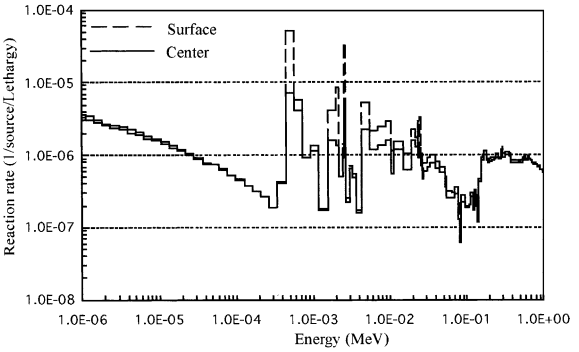

Fig. 3. Energy profile of the ^{63}Cu(n,γ)^{64}Cu reaction rate.

These results indicate that the self-shielding effect is important for predicting the decay heat source in thick copper plates, therefore, sophisticated neutron transport calculation techniques such as MCNP are required.

4.2. Decay heat of SS316

Measured pulse height spectra by WEAS at ≃1 h cooling clearly demonstrate that the main contributor of the decay heat is ^{56}Mn. Discrete peaks corresponding to the beta energy of 1.04 MeV emitted from ^{56}Mn was clearly observed. The high-energy end of the sun-spectrum is equal to the decay Q-value of ^{56}Mn at 3695 keV. This result indicates that ^{56}Mn is the only nuclide that contributes practically to the decay heat. Gradients of decay curves for SS316 samples were also consistent with the expected gradient with a half-life of 2.579 h.

Measured data for all samples were converted to decay heat values at the cooling time of 1 h. The decay heat distribution in the thick SS316 plate and the calculated production rates of ^{56}Mn were shown in Fig. 4. Both experimental and calculated spatial distributions are normalized for comparison so that the spatial average is unity. It is obvious that the spatial distribution by

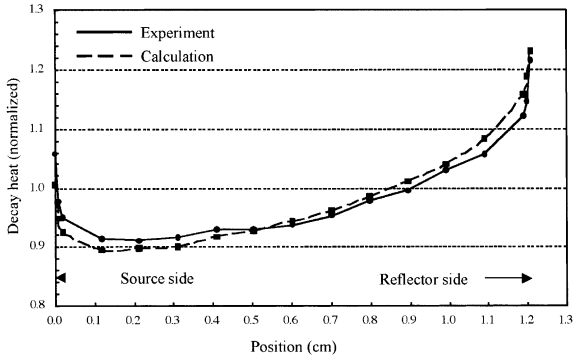

Fig. 2. Comparison of decay heat and ^{64}Cu production rate in the thick copper plate.

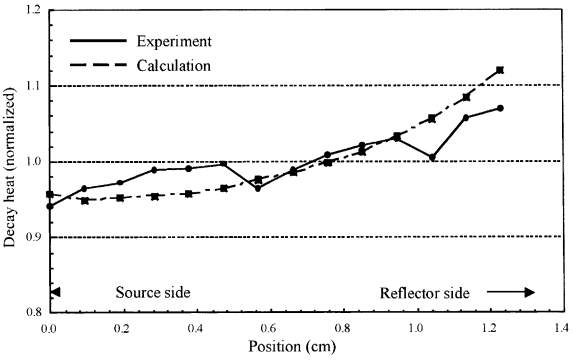

Fig. 4. Comparison of decay heat and ^{56}Mn production rate in the thick SS316 plate.

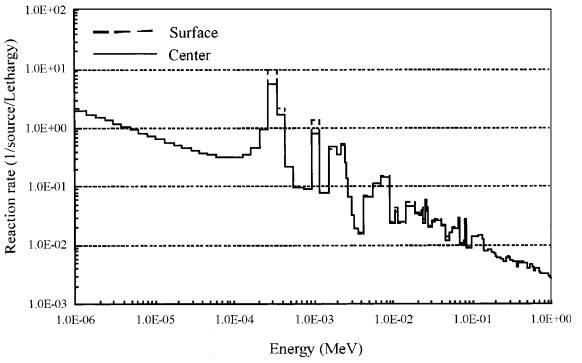

Fig. 5. Energy profile of the $^{55}Mn(n,\gamma)^{56}Mn$ reaction rate.

calculation agrees nicely with the experimental distribution (within $\simeq$10%). The predicted decay heat values averaged in the thick sample plates were compared with the averaged decay heat value of the SS316 plates. The decay heat calculation was conducted with the neutron flux averaged over the thick SS316 plates. C/E values of the decay heat of SS316 were 1.06 when the self-shielding effect of $^{55}Mn(n,\gamma)^{56}Mn$ was included in the calculation and 1.21 when the self-shielding effect of $^{55}Mn(n,\gamma)^{56}Mn$ was not included in the calculation. Two reaction mechanisms of $^{56}Fe(n,p)$ and $^{55}Mn(n,\gamma)$ have comparable contributions for production rates of ^{56}Mn, so the spatial distribution of the production rate of ^{56}Mn is more gentle than that of ^{64}Cu. Nevertheless the self-shielding effects should be treated precisely for the accurate prediction of the decay heat source of SS316.

Fig. 5 shows effective $^{55}Mn(n,\gamma)^{56}Mn$ reaction cross-sections at the two positions, which are derived by dividing the group-wise reaction rates by the group-wise neutron fluxes. The effective cross-section at 300 eV is decreased by nearly 40% due to the self-shielding effect. This is the reason why the reaction rates of the $^{55}Mn(n,\gamma)^{56}Mn$ reaction are small at the center of SS316 plates.

These results indicate that the self-shielding effect is important for predicting the decay heat source in thick SS316 plates, therefore, sophisticated neutron transport calculation techniques such as MCNP should be used.

5. Conclusion

It was confirmed from the experimental results that almost all decay heat originated from ^{64}Cu nuclei was produced by the $^{63}Cu(n,\gamma)$ reactions. The measured decay heat distribution in the thick copper plate suggested an influence of the self-shielding effect. The measured decay heat distribution in the thick copper plate was compared with the predicted values by an MCNP calculation. As a result, the calculated distribution agreed very well with the measured one. C/E values of the decay heat of copper were 1.72 when the self-shielding effect of the $^{63}Cu(n,\gamma)$ reaction was not included in the calculation and 1.15 when the self-shielding effect of $^{63}Cu(n,\gamma)$ reaction was included in the calculation. Consequently, it was concluded that careful treatments of the self-shielding effect were required for calculating the decay heat of copper, and MCNP calculations cold predict the decay heat adequately.

It was also confirmed from the experimental results that almost all decay heat originated from ^{56}Mn nuclei produced by the $^{55}Mn(n,\gamma)$ reactions and $^{56}Fe(n,p)$ reactions. The measured decay heat distribution in the thick SS316 plates suggested a relatively small influence of the self-shielding effect compared with those for the thick copper plates. This is because one of the production reactions of ^{56}Mn is a threshold reaction and the two reaction mechanisms have comparable contributions.

The measured decay heat distribution in the thick SS316 plate was compared with the predicted values by an MCNP calculation. As a result, the calculated distribution agreed very well with the measured one. C/E values of the decay heat of SS316 were 1.06 when the self-shielding effect of $^{55}Mn(n,\gamma)$ was included in the calculation, and 1.21 when the self-shielding effect of $^{55}Mn(n,\gamma)$ was not included in the calculation. Consequently, it was concluded that the self-shielding effect of the $^{55}Mn(n,\gamma)$ reactions were important for calculating the decay heat of manganese-rich stainless steel, and MCNP calculations could predict the decay heat adequately.

Acknowledgements

This report is an account of work undertaken within the framework of the ITER EDA Agreement. The views and opinions expressed herein do not necessarily reflect those of the Parties to the ITER Agreement, the IAEA or any agency thereof. Dissemination of the information included in this paper is governed by the applicable terms of the ITER EDA Agreement. The authors would like to appreciate the task officer, Dr H.W. Bartels for his support for the work. The authors also would like to express their sincere thanks to the operation staff of FNS for their collaboration for the experiment with using FNS.

References

[1] F. Maekawa, M. Wada, C. Konno, Y. Kasugai, Y. Ikeda, Fusion Eng. Des. 51&52 (2000) 809.
[2] M.E. Sawan, H.Y. Khater, H. Iida, R.T. Santro, Fusion Technol. 34 (1998) 1008.
[3] J.F. Briemwister (Ed.), MCNP – A General Monte Carlo *n*-Particle Transport Code, Version 4A, Los Alamos National Laboratory LA-12625-M, 1993.

[4] N.P. Taylor, Y. Ikeda, H.-W. Bartels, G. Cambi, D.G. Ceprga, E.T. Cheng, et al., Fusion Eng. Des. 45 (1999) 75.
[5] F. Maekawa, M. Wada, Y. Ikeda, Nucl. Instrum. and Meth. A 450 (2000) 467.
[6] F. Maekawa, Y. Ikeda, in: Proceedings of the International Conference on Nuclear Data for Science and Technology, May 19–24, Trieste, Italy, 1997, p. 1201.
[7] A.B. Paschneko, H. Wienke, International Atomic Energy Agency, IAEA-NDS-175, 1998.
[8] Y. Seki et al., Japan Atomic Energy Research Institute, JAERI 1301, 1986.
[9] A.B. Paschneko, H. Wienke, J. Kopecky, J.-Ch. Sublet, R.A. Forreset, International Atomic Energy Agency, IAEA-NDS-173, 1998.